

Heterogeneously Catalyzed Diastereoselective Synthesis of 2-Nitro-1,3-di(pyridin-2-yl)propane-1,3-diols

Martin Schulz^a, Katja Wimmer^b, Helmar Görls^b, and Matthias Westerhausen^b

^a Institut für Anorganische und Analytische Chemie, Friedrich-Schiller-Universität Jena, August-Bebel-Straße 2, 07743 Jena, Germany

Current address:

School of Chemical Sciences, Dublin City University, Glasnevin, Dublin 9, Ireland

^b Institut für Anorganische und Analytische Chemie, Friedrich-Schiller-Universität Jena, August-Bebel-Straße 2, 07743 Jena, Germany

Reprint requests to Dr. Martin Schulz. E-mail: martin.schulz@dcu.ie

Z. Naturforsch. **2011**, *66b*, 611–623; received Februar 22, 2011

2-Nitro-1,3-di(pyridin-2-yl)propane-1,3-diols **4a**, **4b** are prepared *via* nitroaldol (Henry) reaction in two separate steps by straightforward procedures. The employment of two solids as catalysts, namely the hydrotalcite Syntal 696[®] and the ion exchange resin Amberlyst A21[®] allows a simple work-up and leads to the diastereoselective formation of the (*R,R*)- and (*S,S*)-isomers. The solid-state structures of **4a**, **4b** as well as of their precursor compounds **3a** and **3b** were determined. Reaction of **4a** with zinc chloride yields a mononuclear zinc chloride complex. To circumvent retro-reactions, trialkylsilyl protective groups are deployed.

Key words: Heterogeneous Catalysis, Nitroaldol Reaction, N,O Ligands, Configuration Determination, Solid-state Structures

Introduction

The demand for custom-tailored metal complexes for example for catalysis or as enzyme-model compounds is a challenge for organic chemists, since this is synonym with the need for custom-tailored ligands [1]. This is particularly important for the development of ligands for homo- and heterodimetallic complexes serving as functional or structural mimics of enzymes. Examples are metallo- β -lactamase [Zn(II), Zn(II)], bovine lens leucine amino peptidase [Zn(II), Zn(II)], alkaline phosphatase [Zn(II), Zn(II)], kidney bean purple acid phosphatase [Zn(II), Fe(III)] or DNA polymerase I [Zn(II), Mg(II)] [2, 3]. Reported mimics are based on phenolate, phthalazine or pyrazolyl linkers as well as cryptands and calix[4]arenes [3–7]. However, most of the used ligands lack the possibility to easily alter the backbone in order to affect the metal-metal distance. Furthermore, often symmetrical ligands are used, even for heterodinuclear complexes, whose syntheses then require elaborate separation procedures. The latter problem was addressed by Roth and coworkers who developed a pathway for the preparation of unsymmetrical ligands for heterodimetallic complexes [8–10]. It is our aim to develop a ligand

preparation pathway which allows the facile and flexible alteration of the ligand backbone. The pathway should allow the introduction of nitrogen and oxygen donor atoms and to facilitate the synthesis of unsymmetrical ligands in order to obtain heterodinuclear complexes. Herein we present the first steps of this ligand preparation pathway. Attention was paid to the structural and spectroscopic investigation of the compounds in order to obtain data for the rational design of metal complexes.

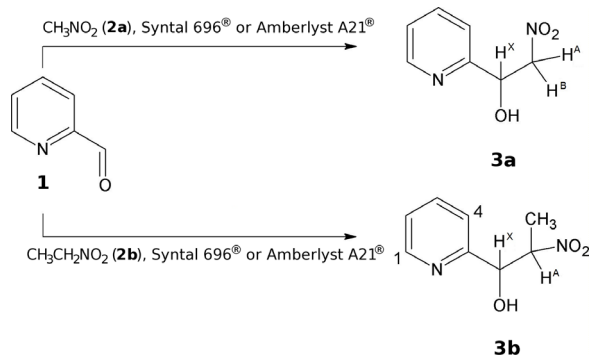
The well-established nitroaldol (Henry) reaction is a possible approach for the construction of ligands [11]. This C–C coupling reaction affords 2-nitroalcohols and represents a valuable access to ligands with nitrogen and oxygen donor sites. For the design of unsymmetrical compounds the reaction conditions should allow sequential C–C coupling steps in order to avoid symmetrical by-products which then have to be separated. Two reported solids seem to be useful catalysts: The Mg-Al-hydrotalcite Syntal 696[®] which is a colorless non-toxic powder, and the weakly basic anion exchange resin Amberlyst A21[®] [12, 13]. With these solids the nitroaldol reactions were sequentially carried out at ambient temperature and with moderate to excellent yields. Additionally the solid catalysts enable re-

actions without acidic work-up and offer a simple catalyst removal procedure. The synthesis of a highly substituted $C(sp^3)$ – $C(sp^3)$ backbone leads to the formation of diastereomers. However, only one diastereomer might be desired for the design of metal complexes, and hence the diastereoselectivity of the ligand preparation pathway was examined. The first part of this work dealt with the development of a modular preparation pathway of 2-nitro-1,3-di(pyridin-2-yl)propane-1,3-diols **4a** and **4b**, while the second part was concerned with finding a suitable protection strategy for the hydroxyl moieties in view of further transformations of the nitro group.

Results and Discussion

The reaction of pyridine-2-carbaldehyde (**1**) in nitromethane (**2a**) in the presence of Syntal 696[®] described by Cwik and coworkers led to the complete conversion of the aldehyde and to the formation of 2-nitro-1-(pyridin-2-yl)ethanol (**3a**) within five hours at r. t. (Scheme 1) [12, 14, 15]. We used Amberlyst A21[®] to catalyze the same reaction with comparable yields within only two hours at r. t.

Compound **3a** can be stored at r. t. under aerobic conditions. Within two weeks the solid turned brown but NMR investigations showed no decomposition products. The filtrate (after crystallization) turned violet within hours. However, dehydration to the nitroalkene was not observed which is in agreement with literature reports [12, 16]. Due to the chiral carbon atom the adjacent methylene protons are diastereotopic, hence showing an ABX spin system in the proton NMR spectrum. The geminal coupling constant is $^2J(H_A, H_B) = 13.2$ Hz, the vicinal coupling constants are $^3J(H_A, H_X) = 4.0$ Hz and $^3J(H_B, H_X) = 8.4$ Hz.



Scheme 1. Nitroaldol reaction of pyridine-2-carbaldehyde (**1**) with nitromethane (**2a**) and nitroethane (**2b**).

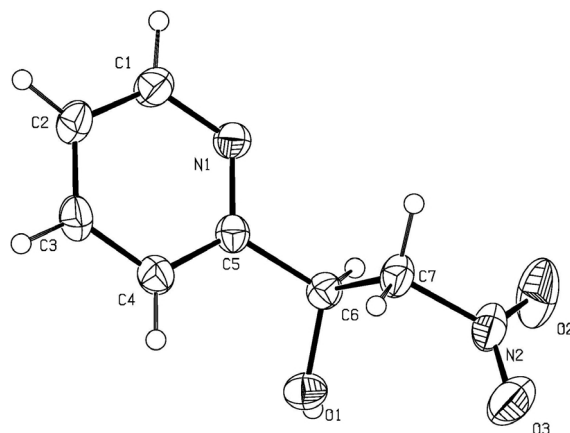
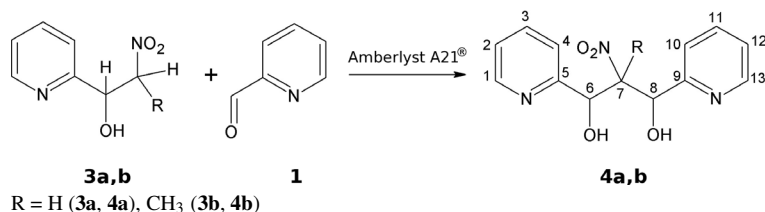


Fig. 1. Molecular structure and numbering scheme of **3a**. The ellipsoids represent a probability of 40%, H atoms are drawn with arbitrary radii. Selected bond lengths (pm) and angles (deg): O1–C6 140.9(2), C6–C7 152.5(2), C5–C6 152.0(2), C6–H6 101.6(17), C7–N2 149.4(2); O1–C6–C5 111.60(14), C5–C6–C7 108.56(14), N2–C7–C6 108.34(14).

The β -nitroalcohol **3a** crystallized in the chiral space group $P2_12_12_1$, even though a measurement of the optical rotation of the product had revealed the racemic nature of **3a** as expected. With the applied $\text{MoK}\alpha$ radiation the determination of the absolute configuration was not possible (Fig. 1). Hydrogen bonds between the OH moiety and the pyridyl nitrogen atom lead to an arrangement of the molecules on a 2-fold screw axis. These interactions are rather strong leading to an $\text{O1}\cdots\text{N1}'$ distance of 272 pm (“'” is used to label atoms of adjacent molecules). All bond lengths and angles are within the expected range [17].

Cwik and coworkers reported also the reaction between nitroethane (**2b**) and **1** in THF in the presence of Syntal 696[®] at 60 °C. The synthesis furnished 2-nitro-1-(pyridin-2-yl)propan-1-ol (**3b**) with excellent yield and a diastereomeric excess of the *erythro* isomer of $de = 30\%$ [12]. We reacted pyridine-2-carbaldehyde (**1**) in a 20-fold molar excess of nitroethane (**2b**) with Amberlyst A21[®] and without any other solvent and obtained **3b** with 39% yield and a 1:1 molar ratio of the *erythro*- and *threo*-isomers. With the employment of Amberlyst A21[®] under neat conditions we obtained the product **3b** with a yield of 79% and a 9:1 ratio of the *threo*:*erythro* isomers ($de = 80\%$). Both isomers can be distinguished by the vicinal coupling constants of the $\alpha\text{-O-CH}^X$ doublet, but since there are three groups capable of forming hydrogen bonds which can affect the conformation, the simple relation $^3J_{anti} > ^3J_{syn}$ is not necessarily diagnostic [18].



Scheme 2. Nitroaldol reaction of pyridine-2-carbaldehyde **1** with the β -nitroalcohols **3a** and **3b**.

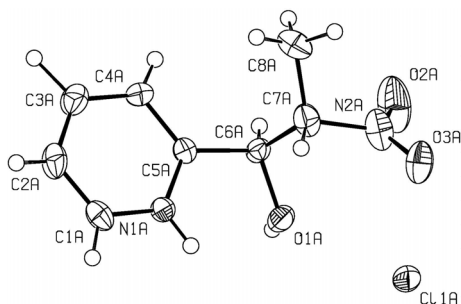


Fig. 2. Molecular structure and numbering scheme of **3b**·HCl. The ellipsoids represent a probability of 40%, H atoms are drawn with arbitrary radii. Selected bond lengths (pm) and angles (deg): O1–C6 140.3(4), C6–C7 154.0(5), C5–C6 150.9(4), C6–H6 91.3(3), C7–N2 148.6(5); O1–C6–C5 110.8(2), C5–C6–C7 108.9(3), N2–C7–C6 107.0(3).

Hence, the assignment of NMR data was made according to the method of Roush and coworkers, who studied the ABX patterns of a vast number of substituted β -hydroxy ketones [19]. They showed that internal hydrogen bonds affect the conformation to a significant extent. Consequently, the larger coupling constant can be assigned to the *threo* isomer ($^3J = 7.2$ Hz), while the smaller coupling constant belongs to the *erythro* isomer ($^3J = 4.0$ Hz). These findings were confirmed by selective NOE experiments.

Slow evaporation of a chloroform solution yielded crystals suitable for X-ray structure analysis in form of the hydrochloride of **3b** (Fig. 2). In the solid state the components of **3b**·HCl form hydrogen bonds Cl \cdots HN and OH \cdots Cl and are arranged along a 2-fold screw axis.

In the crystal of the β -nitroalcohols **3a** and **3b**, hydrogen bonds between the OH moiety and the pyridyl nitrogen atom were found which induce an arrangement of the molecules around a 2-fold screw axis. However, NMR investigations in chloroform solution revealed that hydrogen bond interactions between the OH moiety and the nitro group determine the conformation. In solution, the pyridyl nitrogen atom is not or only to a minor extent involved in hydrogen bonding.

This was shown for **3b** by selective NOE experiments. Irradiation at the NMR frequency of the methyl group resulted in a NOE for the pyridyl protons 1-H and 4-H (Scheme 1). This indicates a free rotation of the pyridyl group and hence no or only weak hydrogen bond interactions.

The proton adjacent to the nitro group of compounds **3a** and **3b** remains acidic allowing further reactions. The selected reaction pathway contains a second nitroaldol reaction step at this position (Scheme 2). This again was achieved with **1** as the substrate, and the conditions for this reaction were investigated. The distinct advantage of using the same aldehyde is of course the formation of a symmetric molecule with a smaller number of possible diastereomers. The reaction was conducted with Amberlyst A21[®] as the catalyst under neat conditions. However, low yields of the diol **4a** were also found with Syntal 696[®] after several weeks. During the reaction a colorless precipitate was formed, which was separated either by washing of the products **4a** and **4b** through a porous frit and retaining the catalyst beads (useful for small amounts up to 3 g) or by separation of the dry powder on a sieve with 0.25 mm mesh size.

Both 2-nitro diols **4a** and **4b** decompose very slowly under atmospheric conditions at r. t., but can be stored for months at -20 °C. It was observed that decomposition of **4a** and **4b** in solution was the faster the more polar the solvent was. This finding is an indicator for an ionic decomposition pathway. Unfortunately, zinc salts such as zinc chloride or zinc perchlorate were found to catalyze the decomposition and the presence of water was found to play a crucial role.

Slow evaporation of ethereal solvents such as diethyl ether or THF yielded crystals suitable for single-crystal X-ray diffraction studies of **4a** and **4b**. Hydrogen bond interactions between the pyridyl nitrogen atoms and the hydroxyl groups were found in the solid-state structure of **4a** and **4b** (Figs. 3 and 4). Four molecules of **4a** are arranged around an inversion center *via* hydrogen bonds and form a globular entity, while molecules **4b** are mutually arranged *via* hydrogen bonding around

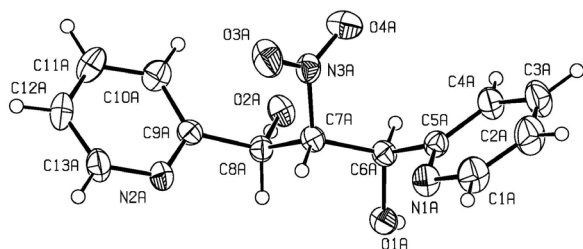


Fig. 3. Molecular structure and numbering scheme of $(R,R)/(S,S)$ -**4a**. The ellipsoids represent a probability of 40%, H atoms are drawn with arbitrary radii. Solvent molecules have been omitted for clarity. Selected bond lengths (pm) and angles (deg): C6–C5 151.6(6), C7–C6 152.7(6), C7–C8 154.2(6), C8–C9 152.2(6), O1–C6 141.5(5), O2–C8 142.1(5), C9–N2 134.0(6), C5–N1 134.6(6); C6–C7–C8 111.9(3), C7–C8–C9 112.9(4), C7–C6–C5 112.8(4), C6–C5–N1 115.8(4), C8–C9–N2 115.6(4).

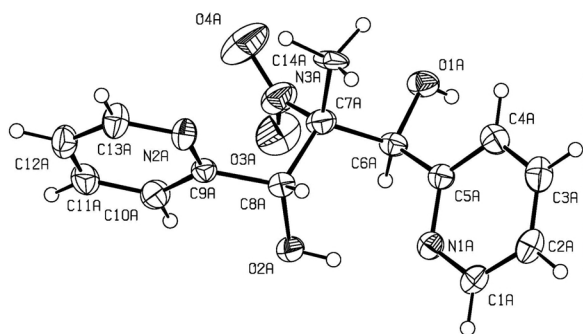


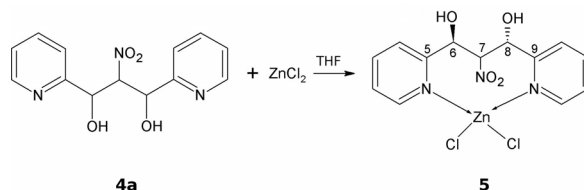
Fig. 4. Molecular structure and numbering scheme of *meso*-**4b**. The ellipsoids represent a probability of 40%, H atoms are drawn with arbitrary radii. Selected bond lengths (pm) and angles (deg): C6–C5 151.9(4), C7–C6 154.9(4), C7–C8 156.7(4), C8–C9 151.2(4), O1–C6 141.6(4), O2–C8 141.0(3), C9–N2 133.5(4), C5–N1 134.3(4); C6–C7–C8 112.3(2), C7–C8–C9 112.2(2), C7–C6–C5 113.0(2), C6–C5–N1 114.7(2), C8–C9–N2 116.8(2).

a two-fold screw axis. The (R,R) - and (S,S) -isomers of **4a** are found in the solid state, and the observed inversion symmetry shows that compound **4a** crystallized as a racemate. In contrast, the *meso*-isomer ($1R,2r,3S$)-**4b** is found in the solid state of **4b**.

A mononuclear zinc(II) chloride complex **5** was obtained when anhydrous zinc chloride was reacted with **4a** in anhydrous THF (Scheme 3). Surprisingly, neither the N,O nor the O,O donor sites became occupied by the zinc atom. Instead, the metal ion was found to be coordinated by the two pyridyl nitrogen atoms in a distorted tetrahedral environment, forming an eight-membered ring. Two THF molecules are hydrogen bonded to the hydroxyl groups with an average O...O distance of 268 pm. The Zn–N bond lengths in **5** are

Table 1. Comparison of the Cl–Zn–Cl angle (deg) with the Zn–Cl and Zn–N bond lengths (pm) of **5** and selected published compounds of the type $(L_2)ZnCl_2$.

Compound	Cl–Zn–Cl	Zn–Cl	Zn–N	Reference
(bipy)ZnCl ₂	117.1	220.4	205.9	[24]
(4-vinyl-py) ₂ ZnCl ₂	118.7	220.9	204.8	[25]
(tmeda)ZnCl ₂	119.0	221.4	209.2	[26]
5	121.16(2)	221.8	206.4	
(4-acetyl-py) ₂ ZnCl ₂	123.6	221.1	205.2	[25]
(4-cyano-py) ₂ ZnCl ₂	125.7	221.3	206.5	[25]



Scheme 3. Reaction of the 2-nitro diol **4a** with zinc chloride and formation of its mononuclear complex **5**.

equal and within the expected range, but with a large N–Zn–N angle of 115.41(6)° [17, 20]. The complexes are present as the $(R,R)/(S,S)$ -isomers, and the crystallographic inversion symmetry reveals that the racemate has crystallized. The Cl–Zn–Cl angle is found to be 121.16(2)° and is comparable with that in several complexes of the type $(L_2)ZnCl_2$ listed in Table 1. Previous investigations of Westerhausen and coworkers showed a linear correlation between the Zn–N bond length and the X–Zn–X angle of tetrahedral complexes of the type L_2ZnX_2 (with L representing a Lewis base with nitrogen donors and X being any monodentate anionic ligand) [21–23]. Short Zn–N bond lengths indicate strong Lewis donor acceptor interactions, and as a result small X–Zn–X angles are found. In the present context the ligand can be considered as strong, which is also supported by the stability of the complex against hydrolysis. No decomposition was observed when **5** was stored under atmospheric conditions for several days.

The complex was found to be stable in anhydrous THF as indicated by NMR investigations. An analysis of the vicinal coupling constants of the O₂NC–H7 proton revealed that no major conformational changes or isomerizations took place. The latter would imply a major change of torsion angles which could be observed by an averaged vicinal coupling constant ³J(H,H) of O₂NC–H7 (*cf.* coupling constants of **4a**). The observed ¹H NMR signal ($\delta = 5.09$) for O₂NC–H7 is a doublet of doublets with ³J = 1.6 Hz and ³J = 10.0 Hz. Similar coupling constants have been calculated from the dihedral angles observed in the crystals

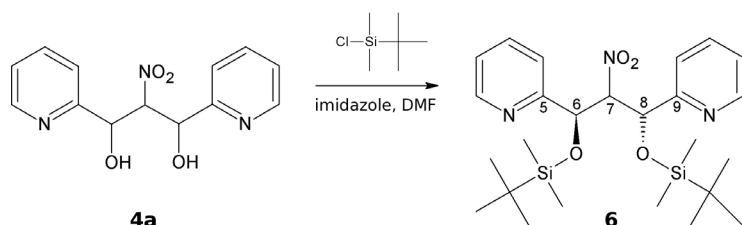
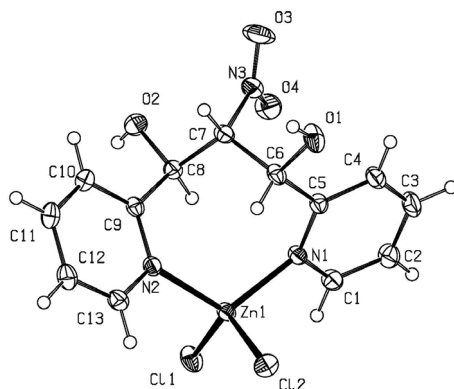
Scheme 4. Protection of **4a** with TBDMSCl.

Fig. 5. Molecular structure and numbering scheme of **5**. The ellipsoids represent a probability of 40%, H atoms are drawn with arbitrary radii. Solvent molecules have been omitted for clarity. Selected bond lengths (pm) and angles (deg): Zn–N1 206.74(15), Zn–N2 206.08(15), C6–C5 151.6(3), C7–C6 155.3(3), C7–C8 153.3(3), C8–C9 151.7(2), O1–C6 140.6(2), O2–C8 140.8(2), C9–N2 134.8(2), C5–N1 134.6(2); C6–C7–C8 115.89(15), C7–C8–C9 109.35(15), C7–C6–C5 113.28(15), C6–C5–N1 116.94(16), C8–C9–N2 117.79(15), N1–Zn–N2 115.41(6), C11–Zn–C12 212.16(2).

(H7A–C7–C6–H6A = 70° and H7A–C7–C8–H8A = 173°). (Fig. 5, H atoms were located by X-ray structure determination). Hypothetical coupling constants (J') were calculated from these angles using an extended Karplus equation introduced by Haasnoot and coworkers [27]. They empirically parameterized the equation, also taking the relative orientations of the non-H-substituents into account, as well as the contributions of the different electronegativities [28]. With this equation two hypothetical coupling constants were calculated: ${}^3J'(\text{H7A}, \text{H6A}) = 1.9 \text{ Hz}$ ($\phi = 70^\circ$) and ${}^3J'(\text{H7A}, \text{H8A}) = 8.7 \text{ Hz}$ ($\phi = 173^\circ$). These results are in excellent agreement with the observed coupling constants. As a result, one can assume that the conformation of complex **5** in THF solution is similar to the one in the solid state, and isomerization equilibria can be excluded.

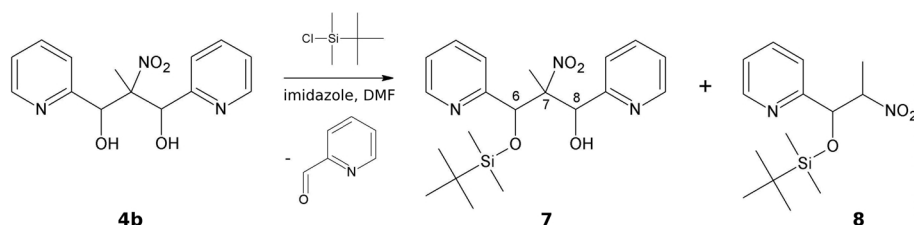
In order to exclude side reactions in the conversion of the nitro group, **4a** was protected with the *tert*-butyldimethylsilyl (TBDMS) protective group. The

Table 2. Comparison of selected NMR data of the compounds **3a**, **3b**, **4a**, **4b**, and **5**. As a convention for compound **5**, 6-H is assigned to the proton with the smaller vicinal coupling constant 3J .

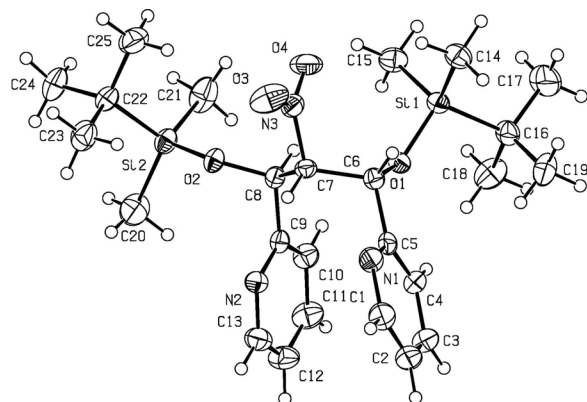
Parameter	3a	3b	4a	4b	5
C-5	156.6	156.4	160.3	156.4	159.6
C-6	70.4	73.3	73.3	74.8	69.7
C-7	80.7	86.6	95.5	98.0	97.6
C-8	–	–	72.5	74.8	69.6
C-9	–	–	160.3	156.4	160.7
HO	4.30	4.59	5.91	4.90	5.92
HO	–	–	6.06	5.40	6.34
6-H	5.45	5.39	5.33	5.32	5.16
7-H	4.79, 4.62	4.84	5.61	–	5.09
8-H	–	–	5.52	5.32	5.49

TBDMS group and its Si–O bond are stable against most oxidizing and reducing agents as well as toward basic conditions [29]. Protection of both hydroxyl moieties of **4a** was achieved in a concentrated DMF solution with TBDMSCl and an excess of imidazole [30]. Due to the hydrophobic and sterically demanding alkyl groups, aqueous work-up led to precipitation of almost pure product **6** with very good yields (Scheme 4).

Two sets of signals are observed in the ${}^1\text{H}$ NMR as well as in the ${}^{13}\text{C}$ NMR spectra of **6**. Cross signals between both OCH moieties in the HMCB spectrum revealed the presence of the (*R,R*) and (*S,S*) isomers. In contrast to compound **4a**, no signals of the *meso*-isomer were observed in the NMR spectra of **6** because the rotation of the bulky TBDMS groups around C6–C7 and C7–C8 is hindered at r. t. Therefore, two doublets are observed for H6 as well as H8 with coupling constants of ${}^3J = 2.2 \text{ Hz}$ and ${}^3J = 9.6 \text{ Hz}$. For the central H atom a doublet of doublets is observed with ${}^3J = 2.0 \text{ Hz}$ and ${}^3J = 9.6 \text{ Hz}$. These findings are in contrast to those of compound **4a** where average vicinal coupling constants were observed (${}^3J = 6.0 \text{ Hz}$). The rotation around the O–Si bonds is also hindered at r. t. NMR spectra show distinct signals for all four Si-bound methyl groups, whereas each *tert*-butyl group appears as a distinct singlet. Table 3 gives an overview over selected chemical shifts of the compounds **4a**, **6** and **5**. No major differences are found.

Scheme 5. Protection of **4b** with TBDMSCl.Table 3. Comparison of selected NMR data (chemical shifts, δ) of the compounds **4a**, **6** and **5**. As a convention for the compounds **5** and **6**, 6-H is assigned to the proton with the smaller vicinal coupling constant 3J .

Parameter	4a	6	5
C-5	160.3	158.6	159.6
C-6	73.3	74.0	69.7
C-7	95.5	96.9	97.6
C-8	72.5	73.2	69.6
C-9	160.3	157.6	160.7
(HO1)	(5.91)	–	(5.92)
(HO2)	(6.06)	–	(6.34)
6-H	5.33	5.10	5.16
7-H	5.61	5.67	5.09
8-H	5.52	5.55	5.49

Fig. 6. Molecular structure and numbering scheme of **6**. The ellipsoids represent a probability of 40%, H atoms are shown with arbitrary radii. Selected bond lengths (pm) and angles (deg): C6–C5 151.9(3), C7–C6 154.3(3), C7–C8 151.9(3), C8–C9 151.2(3), O1–C6 141.4(2), O2–C8 142.7(2), C9–N2 133.7(3), C5–N1 134.2(3); C6–C7–C8 114.75(17), C7–C8–C9 110.84(17), C7–C6–C5 109.62(18), C6–C5–N1 113.82(19), C8–C9–N2 115.36(18).

Crystals suitable for single-crystal X-ray diffraction were obtained by slow solvent evaporation from a solution of **6** in methanol. The crystal structure of **6** (Fig. 6) was solved in space group $P\bar{1}$, and due to crystallographic inversion symmetry, the compound is a racemate. Bond lengths and angles are within the expected range. The Si1–O1–C6 angle of $131.15(13)^\circ$ and the Si2–O2–C8 angle of $126.39(12)^\circ$ are typical

for alkylsilyl ethers and hint at sp^2 -hybridized oxygen atoms.

The same protection condition was applied to **4b**. Aqueous work-up and treatment with pentane afforded 3-(*tert*-butyldimethylsilyloxy)-2-methyl-2-nitro-1,3-di(pyridin-2-yl)propan-1-ol (**7**) as a pentane-insoluble residue with one TBDMS group (Scheme 5).

From the organic phase an oily residue was obtained, which was mainly 2-nitro-1-(pyridin-2-yl)-1-(*tert*-butyldimethylsilyloxy)propane (**8**). This finding indicates that a retroaldol reaction occurred under the applied protection conditions. Due to this fact, the obtained yields of pure **7** were only 30%. The mono-protected silyl ether **7** exhibits three stereogenic centers and can lead to eight possible stereoisomers (four different pairs of enantiomers). NMR investigations have shown that only one pair of enantiomers was obtained. Only a single set of signals with two chemically different pyridyl groups was observed. Stereochemical assignment is complicated, due to the loss of the propyl backbone's vicinal proton-proton coupling. Furthermore, rotation around the C–C single bonds is not fully hindered at r. t. (as observed for compound **6**), thus NOE experiments can only give a rough idea of the obtained isomers. Therefore single-crystal X-ray diffraction was employed to determine the relative configuration of compound **7**. Suitable crystals were obtained by slow solvent evaporation of a diethyl ether solution of **7**. The obtained colorless crystals were uniform in shape and represented almost the whole dissolved mass of **7**. The centrosymmetric space group $C2/c$ with a crystallographic inversion center suggests the presence of a racemate. The relative configuration was determined to be $6S,7S,8R$ and $6R,7R,8S$ (numbering according to Scheme 5). This is in agreement with NOE results in solution. It is noteworthy that the conformation in the solid state is affected by an internal hydrogen bond between O1 and N2 (Fig. 7) with a donor...donor distance of 270 pm.

In order to protect β -nitro alcohol **3b** with TBDMS, a similar protection protocol as employed for com-

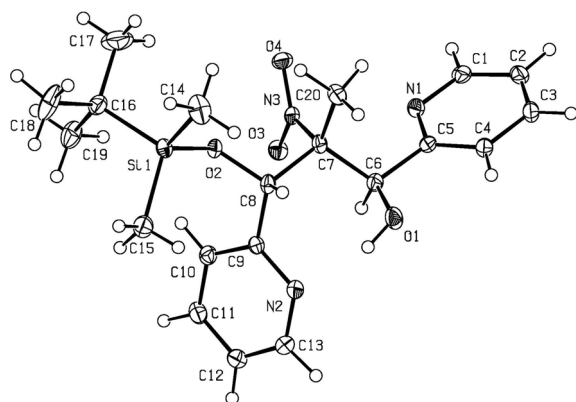
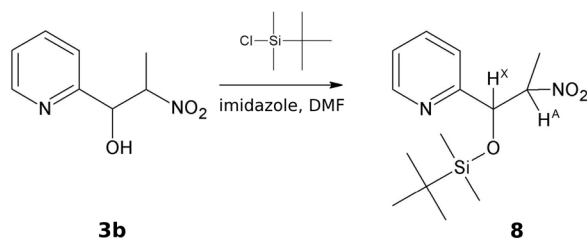


Fig. 7. Molecular structure and numbering scheme of **7**. The ellipsoids represent a probability of 40%. H atoms are shown with arbitrary radii. Selected bond lengths (pm) and angles (deg): C6–C5 151.4(3), C7–C6 155.3(3), C7–C8 156.6(3), C8–C9 152.1(3), O1–C6 141.8(2), O2–C8 141.6(2), C9–N2 135.0(3), C5–N1 134.4(3); C6–C7–C8 111.89(16), C7–C8–C9 117.08(18), C7–C6–C5 112.88(16), C6–C5–N1 114.85(18), C8–C9–N2 115.13(18).



Scheme 6. Protection of **3b** with TBDMSCl.

Compound **6** was used. Aqueous work-up and extraction with diethyl ether afforded pure **8** as a yellowish oil in moderate yield (Scheme 6).

As already described for compound **3b**, the formation of two pairs of enantiomers can be expected. These are (*R,S*)/(*S,R*) or *erythro* and (*R,R*)/(*S,S*) or *threo*, respectively. Both pairs were observed by NMR spectroscopy, and their relative configuration (*erythro* and *threo*) was determined. Surprisingly, the two isomers were found with a ratio of 1.5 : 1 *erythro* : *threo* (de = 20%). The excess of *erythro*-isomer is in contrast to compound **3b** where an excess of the *threo*-isomer was observed. Due to the protected hydroxyl group, the aforementioned assumptions according to Roush (*vide supra*) can not be made [19]. The bulky TBDMS group hinders rotation around the C6–C7 bond as indicated by the observation of two distinct vicinal coupling constants ($^3J(\text{H}^X, \text{H}^A)$) for H^X , assigned as $^3J = 2.8$ Hz (*threo*-**8**) and $^3J = 8.0$ Hz (*erythro*-**8**).

Conclusions

With the solid catalysts Syntal 696[®] and Amberlyst A21[®] a modular synthesis of 1,3-dipyridin-2-yl-propane-1,3-diols has been developed. The first step of the nitroaldol reaction proceeded with very good yields and required only a simple work-up. Consecutive reactions of the intermediate products **3a** and **3b** with pyridine-2-carbaldehyde (**1**) were not observed under the applied conditions, which then allowed the consecutive assembling of unsymmetrically substituted propane-1,3-diols. For example an introduction of oxygen donor sites through reaction with salicylaldehyde or a fine-tuning by the reaction with substituted pyridines are possible. Isomerization can be prevented with employment of the TBDMS protective group, and **4a** was obtained diastereoselectively as (*R,R*)/(*S,S*)-isomers with very good yields. Protection of compound **4b** led with moderate yields to **7**. It is remarkable that by protection of **4b** only one pair of enantiomers out of four possible alternatives was obtained, whose relative configuration could be determined by single-crystal X-ray analysis and was shown to be 1*S*, 2*S*, 3*R* and 1*R*, 2*R*, 3*S*, respectively. This observation gives reason to assume that unsymmetrically substituted propane-1,3-diols may also be received diastereoselectively with the described reaction protocol. Moreover, product **7** comprises an NNO donor set and should be applicable as a di- or tridentate ligand. The use of protecting groups also enables the conversion of the nitro group without any significant side reactions. The products can be used as ligands and ligand precursors [31].

Experimental Section

General remarks. All manipulations were carried out in an argon atmosphere using standard Schlenk techniques. The solvents were dried according to common procedures and distilled under argon. One-dimensional ^1H and ^{13}C NMR spectra were obtained on a Bruker AC 200 (200 MHz), while two-dimensional spectra were obtained on a Bruker AC 400 (400 MHz) spectrometer. Assignment of NMR data was made on the basis of ^1H , ^{13}C , DEPT135, HSQC, HMBC, H,H COSY and selective NOE experiments (numbering according to Scheme 2). Mass spectra were obtained on a Finnigan MAT SSQ 710 system. Peaks in the mass spectra were assigned by comparison of the observed isotopic patterns with the calculated ones. The IR spectra were taken as Nujol mulls between KBr windows, as KBr pellets or neat between KBr windows on a Perkin-Elmer System 2000 FTIR instrument. Melting and decomposition points were

measured on a Reichert-Jung apparatus type 302102 and are uncorrected.

2-Nitro-1-(pyridin-2-yl)ethanol (**3a**)

15 g of Amberlyst A21[®] was added to a solution of pyridine-2-carbaldehyde (**1**, 8.61 g, 0.08 mol) in nitromethane (**2a**, 97.66 g, 1.6 mol). The mixture was stirred for 2 h at r.t. Subsequently, the catalyst beads were removed by filtration, and the filtrate was concentrated to 15 mL on a rotatory evaporator and then left for crystallization at 5 °C over night. The crystalline product was separated from the violet solution by filtration and washed twice with small amounts of cold diethyl ether. A second crop may be obtained by further reduction of the mother liquor's volume and cooling to -20 °C. The product was dried *in vacuo* at r.t. yielding 12.86 g of colorless **3a**. Product **3a** was stored in an argon atmosphere at -20 °C. The excess of nitromethane **2a** could be recovered by distillation and was used for further reactions. Yield 99%; m. p. 70–72 °C. ¹H NMR (CDCl₃): δ = 8.53 (d, *J* = 4.4 Hz, 1H, 1-H), 7.72–7.77 (m, 1H, 3-H), 7.44 (d, *J* = 7.6 Hz, 1H, 4-H), 7.28–7.24 (m, 1H, 2-H), 5.45 (dd, *J* = 3.6 Hz, *J* = 8.4 Hz, 1H, 6-H), 4.76 (dd, *J* = 13.2 Hz, *J* = 4.0 Hz, 1H, 7a-H), 4.62 (dd, *J* = 13.2 Hz, *J* = 8.4 Hz, 1H, 7b-H), 4.3 (s, br, OH). – ¹³C NMR (CDCl₃): δ = 156.6 (q, C-5), 148.9 (t, C-1), 137.4 (t, C-3), 120.9 (t, C-4), 123.6 (t, C-2), 70.4 (t, C-6), 80.7 (s, C-7). – IR (KBr, cm⁻¹): ν = 3078 st (OH), 2842 st, 2736 st, 1600 st (C=N), 1576 st (C=C), 1542 st (N–O), 1478 st, 1440 st, 1415 st, 1378 st, 1333 st, 1291 m, 1224 m, 1200 st, 1154 m, 1113 st, 1079 st, 1039 st. – MS (EI): *m/z* (%) = 169 (42) [M+1]⁺, 121 (92) [M–NO₂]⁺, 108 (100), 93 (99), 78 (98) 51 (57), 39 (28), 27 (25). – C₇H₈N₂O₃ (168.15): calcd. C 50.00, H 4.80, N 16.66; found C 50.04, H 4.72, N 16.69.

2-Nitro-1-(pyridin-2-yl)propan-1-ol (**3b**)

Pyridine-2-carbaldehyde (**1**, 11.78 g, 0.11 mol) was dissolved in nitroethane (**2b**, 8.26 g, 0.11 mol) and 18 g of Amberlyst A21[®] was added. The temperature of the mixture rose to 63 °C within 5 min, while the catalyst's surface became reddish in color. After vigorous stirring for 1 h the mixture became solid and was suspended in 10 mL of methylene chloride. This suspension was stirred over night at r.t. Subsequently, all solid products were dissolved in methylene chloride, and the solution was separated from the catalyst by filtration. The filtrate was reduced on a rotatory evaporator to a fourth of its original volume and left at -20 °C for crystallization. The obtained solid was washed twice with small amounts of methylene chloride and dried *in vacuo* at r.t. yielding 30.00 g of the colorless to greenish product **3b**. Product **3b** was stored in an argon atmosphere at -20 °C. Crystals suitable for single-crystal X-ray diffraction studies were obtained by slow solvent evaporation of a chloro-

form solution of **3b** as the hydrochloride **3b**·HCl. Yield 79%; m. p. 61–62 °C.

threo-2-Nitro-1-(pyridin-2-yl)propan-1-ol. – ¹H NMR (CDCl₃): δ = 8.56–8.54 (m, 1H, 1-H), 7.77–7.72 (m, 1H, 3-H), 7.34 (d, *J* = 7.6 Hz, 1H, 4-H), 7.31–7.26 (m, 1H, 2-H), 5.06 (d, *J* = 7.2 Hz, 1H, 6-H), 4.90 (quint, *J* = 6.8 Hz, 1H, 7-H), 4.59 (s, br, OH), 1.42 (d, *J* = 6.8 Hz, 3H, CH₃). – ¹³C NMR (CDCl₃): δ = 156.5 (q, C-5), 148.7 (t, C-1), 137.5 (t, C-3), 122.2 (t, C-4), 123.8 (t, C-2), 74.6 (t, C-6), 87.4 (t, C-7), 15.4 (p, CH₃).

erythro-2-Nitro-1-(pyridin-2-yl)propan-1-ol. – ¹H NMR (CDCl₃): δ = 8.56–8.54 (m, 1H, 1-H), 7.77–7.72 (m, 1H, 3-H), 7.38 (d, *J* = 8.0 Hz, 1H, 4-H), 7.31–7.26 (m, 1H, 2-H), 5.39 (d, *J* = 4.0 Hz, 1H, 6-H), 4.86–4.81 (m, 1H, 7-H), 4.59 (s, br, OH), 1.40 (d, *J* = 6.4 Hz, 3H, CH₃). – ¹³C NMR (CDCl₃): δ = 156.4 (q, C-5), 148.5 (t, C-1), 137.4 (t, C-3), 121.1 (t, C-4), 123.5 (t, C-2), 73.3 (t, C-6), 86.6 (t, C-7), 12.2 (p, CH₃). – IR (KBr, cm⁻¹): ν = 3108 st (OH), 2946 m, 2909 m, 2842 m, 1598 st (C=N), 1573 m (C=C), 1552 st (N–O), 1547 st (N–O), 1440 st, 1388 st, 1368 st, 1332 m, 1310 m, 1286 m, 1268 m, 1250 m, 1213 m, 1150 m, 1136 m, 1075 m, 1054 m, 1007 st, 997 st. – MS (EI): *m/z* (%) = 183 (36) [M+1]⁺, 136 (100) [M–NO₂]⁺, 118 (89), 108 (82), 78 (45). – C₈H₁₀N₂O₃ (182.18): calcd. C 52.74, H 5.53, N 15.38; found C 52.64, H 5.65, N 15.24.

rac-2-Nitro-1,3-di(pyridin-2-yl)propane-1,3-diol (**4a**)

Nitroalcohol **3a** (13.00 g, 0.08 mol) was dissolved in pyridine-2-carbaldehyde (**1**, 8.61 g, 0.08 mol), and 13.40 g of Amberlyst A21[®] was added, while the internal temperature markedly increased. After stirring for 1 h, 20 mL of methylene chloride was added, and the obtained suspension was stirred over night at r.t. Subsequently, the solids were removed by filtration and carefully dried. Separation of the catalyst beads from product **4a** was achieved with a 0.25 mm mesh sieve. The obtained colorless powder was washed twice with small amounts of methylene chloride and dried *in vacuo* at r.t. yielding 15.86 g of **4a**. Product **4a** was stored in an argon atmosphere at -20 °C. Crystals suitable for single crystals X-ray analysis were obtained by slow solvent evaporation from diethyl ether or THF solutions. Separation of small amounts of **4a** from the catalyst was achieved by transferring the suspension to a porous frit *via* Pasteur pipette. Yield 72%; m. p. 116–118 °C (dec.). – ¹H NMR (CD₃OD): δ = 8.41 (d, *J* = 4.8 Hz, 1H, 1-H), 8.35 (d, *J* = 4.8 Hz, 1H, 13-H), 7.70 (ddd, *J* = 1.6 Hz, *J* = 7.6 Hz, 1H, 11-H), 7.64 (ddd, *J* = 1.6 Hz, *J* = 8.0 Hz, 1H, 3-H), 7.49 (d, *J* = 7.6 Hz, 1H, 10-H), 7.34 (d, *J* = 8.0 Hz, 1H, 4-H), 7.19 (m, 1H, 2-H), 7.19 (m, 1H, 12-H), 6.07 (s, br, OH), 5.91 (s, br, OH), 5.61 (t, *J* = 6.0 Hz, 1H, 7-H), 5.52 (d, *J* = 6.0 Hz, 1H, 8-H), 5.33 (d, *J* = 5.6 Hz, 1H, 6-H). – ¹³C NMR (CD₃OD): δ = 160.3 (q, C-5), 160.2 (q, C-9), 149.8 (t, C-1), 149.6 (t, C-13), 138.3 (t, C-11), 138.2 (t, C-3), 123.4 (t, C-10), 123.2 (t, C-4), 124.3

(t, C-2), 124.1 (t, C-12), 95.5 (t, C-7), 72.5 (t, C-8), 73.3 (t, C-6). – IR (KBr, cm^{-1}): $\nu = 3114$ st br (OH), 2846 st (CH), 1597 st (C=N), 1574 st, 1541 st (N–O), 1476 st, 1440 st, 1367 st, 1309 m, 1277 m, 1261 m, 1216 m, 1155 m, 1008 st. – MS (DEI): m/z (%) = 275 (76) $[\text{M}]^-$, 229 (16) $[\text{M}-\text{NO}_2]^+$, 211 (57), 149 (13), 134 (15), 122 (33), 108 (42), 106 (28), 93 (20), 78 (100). – $\text{C}_{13}\text{H}_{13}\text{N}_3\text{O}_4$ (275.26): calcd. C 56.72, H 4.76, N 15.15; found C 56.50, H 4.75, N 15.27.

rac-2-Methyl-2-nitro-1,3-di(pyridin-2-yl)propane-1,3-diol (**4b**)

Nitroalcohol **3b** (12.00 g, 0.07 mol) was dissolved in pyridine-2-carbaldehyde (**1**, 7.10 g, 0.07 mol), and 9.50 g of Amberlyst A21[®] was added, while the internal temperature markedly increased. Stirring over night afforded a colorless solid, which was suspended in diethyl ether and stirred for additional 3 h at r. t. Subsequently, the solids were removed by filtration and carefully dried. The ethereal filtrate was reduced to half of its original volume and left at -20 °C, while further product precipitated. Separation of the catalyst beads was achieved with a 0.25 mm mesh sieve. The combined products were washed twice with small amounts of diethyl ether and dried *in vacuo* at r. t. yielding 9.92 g of product **4b**, which was then stored in an argon atmosphere at -20 °C. Crystals suitable for single-crystal X-ray diffraction were obtained by slow solvent evaporation of solution of **4b** in diethyl ether. Separation of small amounts of **4b** from the catalyst was achieved by transferring the suspension to a porous frit *via* Pasteur pipette. Yield 49%; m.p. 111–113 °C. – ^1H NMR (CD_2Cl_2): $\delta = 8.60$ – 8.45 (m, 2H, 1-H, 13-H), 7.80–7.72 (m, 2H, 3-H, 11-H), 7.44 and 7.52 (d, $J = 8.0$ d, 7.6 Hz, 2H, 2-H, 10-H), 7.39–7.28 (m, 2H, 2-H, 12-H), 5.32 (s, 2H, 6-H, 8-H), 1.40 (s, 3H, CH_3). – ^{13}C NMR (CD_2Cl_2): $\delta = 156.5$ and 156.3 (q, C-5, C-9), 148.7 and 148.2 (t, C-1, C-13), 137.5 and 137.4 (t, C-3, C-11), 123.9 and 123.7 (t, C-2, C-10), 122.7 and 122.4 (t, C-2, C-12), 98.2 (q, C-7), 74.9 and 74.7 (t, C-6, C-8), 14.4 (p, CH_3). – IR (Nujol, cm^{-1}): $\nu = 3137$ m, br (OH), 1597 m (C=N), 1539 st (N–O), 1344 m, 1315 m, 1116 m, 1065 st, 1002 m. – MS (FAB in nba): m/z (%) = 290 (80) $[\text{M}+1]^+$, 243 (25) $[\text{M}-\text{NO}_2]^+$, 225 (18), 183 (84), 136 (96), 118 (55), 108 (80), 79 (100). – $\text{C}_{14}\text{H}_{15}\text{N}_3\text{O}_4$ (289.27): calcd. C 58.06, H 5.23, N 14.53; found C 58.13, H 5.19, N 14.71.

[*rac*-2-Nitro-1,3-di(pyridin-2-yl)propane-1,3-diol dichloro zinc]-2 THF (**5**)

Compound **4a** (150 mg, 0.5 mmol) and anhydrous zinc chloride (126 mg, 0.9 mmol) were dissolved in 3 mL of anhydrous THF in an argon atmosphere. The yellowish solution was stirred over night at r. t. and then left for crystallization at -20 °C for several weeks. The formed crystals were separated by filtration and carefully washed with cold

anhydrous THF, yielding 91 mg of complex **5**. The complex was stable for several days under atmospheric conditions. Yield 30%; 95 °C (loss of THF), 107–112 °C (dec.). – ^1H NMR ($[\text{D}_8]\text{THF}$): $\delta = 9.01$ (d, $J = 4.8$ Hz, 1H, 13-H), 8.96 (d, $J = 4.8$ Hz, 1H, 1-H), 8.21 (t, $J = 7.6$ Hz, 1H, 11-H), 8.13 (d, $J = 8.0$ Hz, 1H, 10-H), 8.07 (t, $J = 7.6$ Hz, 1H, 3-H), 7.70–7.67 (m, 1H, 12-H), 7.76 (d, $J = 8.0$ Hz, 1H, 4-H), 7.66–7.63 (m, 1H, 2-H), 6.34 (s, br, HO–(C-8)), 5.92 (s, br, HO–(C-6)), 5.49 (dd, $J = 9.6$ Hz, $J = 2.4$ Hz, 1H, 8-H), 5.16 (s, 1H, 6-H), 5.09 (dd, $J = 10.0$ Hz, $J = 1.6$ Hz, 1H, 7-H). – ^{13}C NMR ($[\text{D}_8]\text{THF}$): $\delta = 160.7$ (q, C-9), 159.6 (q, C-5), 148.7 (t, C-13), 148.6 (t, C-1), 140.7 (t, C-11), 139.9 (t, C-3), 123.6 (t, C-10), 124.7 (t, C-12), 124.5 (t, C-2), 123.5 (t, C-4), 69.7 (t, C-6), 97.6 (t, C-7), 69.6 (t, C-8). – IR (KBr, cm^{-1}): $\nu = 3210$ m, br (OH), 3055 m, 1606 st (C=N), 1573 m (C=C), 1556 st (N–O), 1482 m, 1327 m, 1085 m, 1025 st. – MS (FAB in nba): m/z (%) = 374 (26) $[\text{M}-\text{Cl}]^+$, 338 (16) $[\text{M}-2\text{Cl}-\text{H}]^+$, 276 (100) $[\text{M}-\text{ZnCl}_2+\text{H}]^+$, 242 (11), 229 (18), 211 (50). – $\text{C}_{21}\text{H}_{29}\text{Cl}_2\text{N}_3\text{O}_6\text{Zn}$ (555.79): calcd. C 45.38, H 5.26, N 7.56; found C 45.57, H 5.10, N 7.65.

2-Nitro-1-(pyridin-2-yl)-1-(*tert*-butyldimethylsilyloxy)propane (**8**)

tert-Butyldimethylsilylchloride (5.99 g, 40 mmol) was suspended in 8 mL of DMF and cooled in an ice bath. Subsequently, solid imidazole (4.85 g, 71 mmol) was carefully added, and the mixture was stirred for 15 min. A freshly prepared solution of nitroalcohol **3b** in 10 mL of DMF was added, and the greenish solution was stirred for 20 h at r. t., while the color slowly turned yellow. Subsequently, DMF was removed *in vacuo* (40 °C). The obtained hygroscopic precipitate was stirred in 50 mL of water for 2 h, while an oil segregated from the aqueous solution. The oil was extracted three times with 10 mL of diethyl ether each, and the phases were separated. Drying of the organic phase over sodium sulfate and removal of the solvent *in vacuo* afforded product **8** as a yellowish oil with high purity. Yield 59%.

threo-**8**. – ^1H NMR (CDCl_3): $\delta = 8.52$ (m, 1H, 1-H), 7.73–7.68 (m, 1H, 3-H), 7.19–7.16 (m, 1H, 2-H), 7.46 (d, $J = 8.0$ Hz, 1H, 4-H), 5.54 (d, $J = 2.8$ Hz, 1H, 6-H), 4.96–4.94 (m, 1H, 7-H), 1.24 (d, $J = 6.8$ Hz, 3H, CH_3), 0.77 (s, 9H, *tert*-butyl), -0.02 (s, 3H, SiCH_3), -0.26 (s, 3H, SiCH_3). – ^{13}C NMR (CDCl_3): $\delta = 159.5$ (q, C-5), 149.0 (t, C-1), 136.7 (t, C-3), 122.8 (t, C-2), 120.7 (t, C-4), 86.4 (t, C-7), 76.5 (t, C-6), 25.7 (p, *tert*-butyl), 15.7 (p, CH_3), 18.0 (q, *tert*-butyl), -5.7 (p, SiCH_3), -4.9 (p, SiCH_3).

erythro-**8**. – ^1H NMR (CDCl_3): $\delta = 8.52$ (m, 1H, 1-H), 7.73–7.68 (m, 1H, 3-H), 7.24–7.21 (m, 1H, 2-H), 7.42 (d, $J = 7.6$ Hz, 1H, 4-H), 5.07 (d, $J = 8.0$ Hz, 1H, 6-H), 4.84–4.76 (m, 1H, 7-H), 1.28 (d, $J = 6.8$ Hz, 3H, CH_3), 0.88 (s, 9H, *tert*-butyl), -0.01 (s, 3H, SiCH_3), -0.13 (s, 3H, SiCH_3). – ^{13}C NMR (CDCl_3): $\delta = 158.9$ (q, C-5), 148.9 (t, C-1), 137.0 (t, C-3), 123.4 (t, C-2), 121.8 (t, C-4), 88.5 (t, C-7), 78.0 (t,

C-6), 25.4 (p, *tert*-butyl), 17.9 (q, *tert*-butyl), 10.5 (p, CH₃), –5.7 (p, SiCH₃), –4.9 (p, SiCH₃). – IR (neat, cm^{–1}): ν = 3057 w, 2956 st, 2931 st, 2895 m, 2859 st, 1681 w, 1590 st (C=N), 1554 st (N–O), 1472 st, 1437 st, 1390 st, 1362 st, 1255 st, 1150 st, 1102 st, 1086 st, 1063 st, 1043 m, 1025 st, 1006 m. – MS (DEI): m/z (%) = 297 (14) [M+1]⁺, 281 (4) [M–CH₃]⁺, 250 (12) [M–NO₂]⁺, 239 (100) [M–*tert*-butyl]⁺, 222 (40), 208 (19), 192 (34), 182 (72), 178 (50), 165 (13), 132 (23), 118 (21), 104 (15). – C₁₄H₂₄N₂O₃Si (296.44): calcd. C 56.72, H 8.16, N 9.45; found C 56.39, H 8.16, N 9.69.

rac-2-Nitro-1,3-di(pyridin-2-yl)-1,3-di(*tert*-butyldimethylsilyloxy)propane (**6**)

tert-Butyldimethylsilylchloride (24.40 g, 0.16 mol) was suspended in 28 mL of DMF and cooled in an ice bath. Subsequently, solid imidazole (20.00 g, 0.29 mol) was carefully added, and the mixture was stirred for 15 min. To the mixture, a suspension of compound **4a** (15.50 g, 0.056 mol) in 30 mL of DMF was added. The brownish solution was stirred for 28 h at r. t., while a colorless solid precipitated. The precipitate was separated by filtration and then stirred for 2 h in 80 mL of water yielding a fluffy colorless solid, which again was filtered off. The DMF filtrate was concentrated at 40 °C and 1 · 10^{–2} mbar until a solid precipitated (one third of the original volume). This suspension was stirred for 2 h in 100 mL of water and the obtained fluffy precipitate was collected by filtration. The combined solid products were thoroughly washed with water and dried *in vacuo*, yielding 23.10 g of the colorless crystalline product **6** which was pure and stored under atmospheric conditions at r. t. Crystals suitable for single-crystal X-ray diffraction were obtained by slow solvent evaporation from a methanol solution. Yield 82%; m. p. 84–85 °C. – ¹H NMR (CDCl₃): δ = 8.50 (d, J = 4.4 Hz, 1H, 1-H), 8.42 (d, J = 4.4 Hz, 1H, 13-H), 7.54 (t, J = 7.6 Hz, 1H, 11-H), 7.38 (t, J = 7.6 Hz, 1H, 3-H), 7.30 (d, J = 8.0 Hz, 1H, 10-H), 7.12–7.09 (m, 1H, 12-H), 7.06–7.03 (m, 1H, 2-H), 6.95 (d, J = 8.0 Hz, 1H, 4-H), 5.67 (dd, J = 9.6 Hz, J = 2.0 Hz, 1H, 7-H), 5.55 (d, J = 9.6 Hz, 1H, 8-H), 5.10 (d, J = 2.2 Hz, 1H, 6-H), 0.92 (s, 9H, *tert*-butyl), 0.67 (s, 9H, *tert*-butyl), –0.00 (s, 3H, CH₃), –0.05 (s, 3H, CH₃), –0.23 (s, 3H, CH₃), –0.35 (s, 3H, CH₃). – ¹³C NMR (CDCl₃): δ = 158.6 (q, C-5), 157.6 (q, C-9), 148.8 (t, C-13), 148.0 (t, C-1), 136.6 (t, C-11), 136.4 (t, C-3), 124.1 (t, C-10), 123.3 (t, C-12), 122.3 (t, C-2), 120.9 (t, C-4), 96.8 (t, C-7), 74.0 (t, C-6), 73.2 (t, C-8), 25.7 (p, *tert*-butyl), 25.4 (p, *tert*-butyl), 18.1 (q, *tert*-butyl), 17.9 (q, *tert*-butyl), –5.5 (p, CH₃), –5.6 (p, CH₃), –5.2 (p, CH₃), –5.0 (p, CH₃). – IR (KBr, cm^{–1}): ν = 2957 st, 2929 st, 2886 m, 2856 st, 1590 st (C=N), 1573 m (C=C), 1554 st (N–O), 1472 st, 1435 m, 1397 m, 1360 m, 1338 m, 1317 m, 1261 st, 1136 st, 1096 st, 1083 st, 1046 m, 1006 m. – MS (DEI): m/z (%) = 504 (9) [M]⁺, 457 (7) [M–NO₂]⁺, 446 (46) [M–*tert*-butyl]⁺, 399 (33) [M–

tert-butyl]⁺, 339 (20), 325 (23), 222 (100), 194 (22), 182 (35), 178 (51), 165 (69). – C₂₅H₄₁N₃O₄Si₂ (503.78): calcd. C 59.60, H 8.20, N 8.34; found C 59.76, H 8.27, N 8.24.

3-(*tert*-Butyldimethylsilyloxy)-2-methyl-2-nitro-1,3-di(pyridin-2-yl)propan-1-ol (**7**)

tert-Butyldimethylsilylchloride (755 mg, 5.0 mmol) was suspended in 0.8 mL of DMF and cooled in an ice bath. Subsequently, solid imidazole (588 mg, 8.7 mmol) was carefully added, and the mixture was stirred for 15 min. To this mixture, a freshly prepared suspension of compound **4b** (500 mg, 1.7 mmol) in 1 mL of DMF was added. The brownish suspension was stirred for 28 h at r. t. Subsequently, the solvent was removed *in vacuo* at 40 °C and 1 · 10^{–2} mbar. The obtained oily residue was stirred in 5 mL of water for 2 h. The aqueous phase was removed with a pipette, and the oily residue was stirred in 5 mL of pentane yielding a colorless precipitate. The precipitate was collected on a filter and dried *in vacuo* yielding 200 mg of product **7** which is stable under atmospheric conditions at r. t. Crystals suitable for single-crystal X-ray diffraction were obtained by slow solvent evaporation of a solution of **7** in diethyl ether. – Yield 30%; m. p. 107–108 °C. – ¹H NMR (CDCl₃): δ = 8.49–8.46 (m, 2H, 1-H, 13-H), 7.83 (t, J = 7.2 Hz, 1H, 3-H), 7.70 (t, J = 7.2 Hz, 1H, 11-H), 7.57 (d, J = 7.6 Hz, 1H, 4-H), 7.46 (d, J = 8.4 Hz, 1H, 10-H), 7.34–7.32 (m, 1H, 2-H), 7.19–7.17 (m, 1H, 12-H), 5.20 (s, 1H, 6-H), 5.12 (s, 1H, 8-H), 5.00 (s, broad, OH), 1.45 (s, 3H, CH₃), 0.89 (s, 9H, *tert*-Bu), 0.08 (s, 3H, SiCH₃), –0.35 (s, 3H, SiCH₃). – ¹³C NMR (CDCl₃): δ = 159.2 (q, C-5), 157.6 (q, C-9), 146.8 (t, C-1), 148.0 (t, C-13), 137.5 (t, C-3), 137.5 (t, C-11), 124.0 (t, C-4), 123.7 (t, C-2), 122.8 (t, C-12), 121.8 (t, C-10), 97.3 (q, C-7), 78.2 (t, C-6), 74.0 (t, C-8), 25.5 (p, *tert*-butyl), 17.9 (q, *tert*-butyl), 16.0 (p, CH₃), –5.2 (p, SiCH₃), –4.5 (p, SiCH₃). – IR (KBr, cm^{–1}): ν = 3200–2600 m broad (OH), 3148 m, 1597 m (C=N), 1590 st (C=N), 1573 m (C=C), 1543 st (N–O), 1407 m, 1312 m, 1293 m, 1269 m, 1252 m, 1114 st, 1084 st, 1069 st, 1004 m. – MS (DEI): m/z (%) = 404 (100) [M]⁺, 357 (8) [M–NO₂]⁺, 346 (28) [M–*tert*-butyl]⁺, 299 (27), 250 (40), 225 (25), 192 (61), 182 (21), 165 (18), 118 (14), 78 (17). – C₂₀H₂₉N₃O₄Si (403.55): calcd. C 59.53, H 7.24, N 10.41; found C 59.76, H 7.42, N 10.15.

X-Ray structure determination

The intensity data for the compounds were collected on a Nonius KappaCCD diffractometer using graphite-monochromatized MoK α radiation. Data were corrected for Lorentz and polarization effects but not for absorption [32,33]. The structures were solved by Direct Methods (SHELXS) [34] and refined by full-matrix least-squares techniques against F_o^2 (SHELXL-97) [35]. All non-hydrogen atoms were refined anisotropically [35]. Structure represen-

Table 4. Crystallographic data.

Compound	3a	3b-HCl	4a	4b	5	6	7
Formula	C ₇ H ₈ N ₂ O ₃	C ₈ H ₁₁ ClN ₂ O ₃	C ₁₃ H ₁₃ N ₃ O ₄ ·0.25 C ₄ H ₁₀ O ^b	C ₁₄ H ₁₅ N ₃ O ₄	C ₂₁ H ₂₉ Cl ₂ N ₃ O ₆ Zn	C ₂₅ H ₄₁ N ₃ O ₄ Si ₂	C ₂₀ H ₂₉ N ₃ O ₄ Si
M _r , g mol ⁻¹	168.15	218.64	297.83	289.29	555.74	503.79	403.55
T, °C	-90(2)	-90(2)	-90(2)	-90(2)	-90(2)	-90(2)	-140(2)
Crystal system	orthorhombic	monoclinic	triclinic	monoclinic	monoclinic	triclinic	monoclinic
Space group	P2 ₁ 2 ₁ 2 ₁	P2 ₁ /n	P1	P2 ₁ /c	P2 ₁ /c	P1	C2/c
a, pm	714.50(5)	1268.99(5)	1170.30(12)	1182.18(4)	940.90(2)	740.37(4)	2144.97(9)
b, pm	971.28(7)	890.25(4)	1222.93(15)	2197.76(9)	2104.72(3)	1327.86(11)	1925.24(8)
c, pm	1144.61(6)	1842.18(8)	1229.90(16)	1170.01(5)	1312.68(2)	1587.10(14)	1193.83(6)
α, deg	90	90	74.350(4)	90	90	70.372(3)	90
β, deg	90	101.768(3)	75.045(7)	114.201(2)	107.327(1)	84.549(5)	116.901(3)
γ, deg	90	90	80.880(8)	90	90	84.682(5)	90
V, Å ³	794.34(9)	2037.40(15)	1630.1(3)	2772.69(19)	2481.57(7)	1459.91(19)	4396.5(3)
Z	4	8	4	8	4	2	8
D _x , g cm ⁻³	1.41	1.43	1.21	1.39	1.49	1.15	1.22
μ(MoK _α), cm ⁻¹	1.1	3.6	0.9	1.0	12.5	1.5	1.4
Measured data	5344	13905	10604	19614	18099	10124	14988
Unique data/R _{int}	1830/0.0372	4651/0.0600	7168/0.0359	6345/0.0754	5668/0.0291	6631/0.0437	5028/0.0963
Data with I ≥ 2σ(I)	1397	3092	3800	3532	4811	3707	2937
R ₁ [I ≥ 2σ(I)] ^a	0.0391	0.0638	0.1141	0.0745	0.0313	0.0546	0.0518
wR ₂ (all data, on F ²) ^a	0.1010	0.1778	0.3553	0.2375	0.0788	0.1323	0.1109
GoF (S) ^b	1.018	1.070	1.020	1.039	1.003	0.980	0.993
Δρ _{int} (max/min), e Å ⁻³	0.143/-0.156	0.950/-0.425	0.887/-0.546	1.370/-0.410	0.779/-0.394	0.249/-0.302	0.294/-0.312
CCDC no.	773156	773157	773158	773159	773160	773161	773162

^a $R_1 = \frac{\sum |F_o| - |F_c|}{\sum |F_o|}$, $wR_2 = \frac{\sum w(F_o^2 - F_c^2)^2}{\sum w(F_o^2)^2}$, $w = [\sigma^2(F_o^2) + (aP)^2 + bP]^{-1}$, where $P = (\max(F_o^2, 0) + 2F_c^2)/3$; ^b $GoF = \frac{\sum w(F_o^2 - F_c^2)^2}{(n_{obs} - n_{param})^{1/2}}$; ^c C₄H₁₀O is diethyl ether.

tations: XP (Siemens Analytical X-ray Instruments, Inc.). The hydrogen atoms for compound **3a**, H1–H4, H6 and H8 of **3b**-HCl, and the hydrogen atoms of the hydroxy groups O1, O2 of **4b** and **5** were located in difference Fourier syntheses and refined isotropically. All other hydrogen atoms were included at calculated positions with fixed displacement parameters. The quality of the data of **4a** is not sufficient to give good *R*-values but the esd values obtained for bond lengths and angles are good.

CCDC 773156–773162 contains the supplementary crystallographic data for this paper. These data can be obtained

free of charge from The Cambridge Crystallographic Data Centre via www.ccdc.cam.ac.uk/data_request/cif.

Acknowledgements

This work was supported by the Deutsche Forschungsgemeinschaft (DFG, Bonn-Bad Godesberg, Germany) and the Fonds der Chemischen Industrie (Frankfurt/Main, Germany). We thank Süd-Chemie AG (Munich, Germany) for putting the hydrotalcite Syntal 696® to our disposal. The authors thank M. Friedrich for fruitful discussions on the NOE experiments.

- [1] G. Parkin, *Chem. Rev.* **2004**, *104*, 699–768.
- [2] D. E. Wilcox, *Chem. Rev.* **1996**, *96*, 2435–2458.
- [3] H. B. Kraatz, N. Metzler-Nolte (Eds.), *Concepts and Models in Bioinorganic Chemistry*, Wiley-VCH, Weinheim, **2006**.
- [4] A. Erxleben, J. Hermann, *J. Chem. Soc., Dalton Trans.* **2000**, *4*, 569–575.
- [5] C. Belle, I. Gautier-Luneau, L. Karmazin, J.-L. Pierre, S. Albedyhl, B. Krebs, M. Bonin, *Eur. J. Inorg. Chem.* **2002**, 3087–3090.
- [6] T. Koike, M. Inoue, E. Kimura, M. Shiro, *J. Am. Chem. Soc.* **1996**, *118*, 3091–3099.
- [7] F. Meyer, P. Rutsch, *Chem. Commun.* **1998**, 1037–1038.
- [8] A. Roth, E. T. Spielberg, W. Plass, *Inorg. Chem.* **2007**, *46*, 4362–4364.
- [9] A. Roth, A. Buchholz, M. Rudolph, E. Schütze, E. Kothe, W. Plass, *Chem. Eur. J.* **2008**, *14*, 1571–1583.
- [10] A. Roth, W. Plass, *Angew. Chem.* **2008**, *120*, 7700–7703; *Angew. Chem. Int. Ed.* **2008**, *47*, 7588–7591.
- [11] L. Henry, *Compt. Rend. Hebd. Séances Acad. Sci.* **1895**, *120*, 1265–1268.
- [12] A. Cwik, A. Fuchs, Z. Hell, J. M. Clacens, *Tetrahedron*, **2005**, *61*, 4015–4021.
- [13] R. Ballini, G. Bosica, *J. Org. Chem.* **1994**, *59*, 5466–5467.
- [14] K. W. Merz, H. J. Janssen, *Arch. Pharm.* **1964**, *297*, 10.
- [15] F. Zymalkowski, *Arch. Pharm.* **1955**, *52*–54.
- [16] B. M. Choudary, M. L. Kantam, B. Kavita, *J. Mol. Catal. A: Chem.* **2001**, *169*, 193–197.
- [17] F. H. Allen, O. Kennard, D. G. Watson, L. Brammer, A. G. Orpen, R. Taylor, *J. Chem. Soc., Perkin Trans. 2*, **1987**, S1–S19.
- [18] L. M. Jackman, S. Sternhell, *Applications of Nuclear Magnetic Resonance in Organic Chemistry*, 2nd. ed., Pergamon Press: Oxford, U. K., **1969**.
- [19] W. R. Roush, T. D. Bannister, M. D. Wendt, M. S. Van-Nieuwenhze, D. J. Gustin, G. J. Dilley, G. C. Lane, K. A. Scheidt, W. J. Smith, *J. Org. Chem.* **2002**, *67*, 4284–4289.
- [20] A. G. Orpen, L. Brammer, F. H. Allen, O. Kennard, D. G. Watson, R. Taylor, *J. Chem. Soc., Dalton Trans.* **1989**, S1–S83.
- [21] M. Westerhausen, B. Rademacher, W. Schwarz, *J. Organomet. Chem.* **1992**, *427*, 275–287.
- [22] M. Westerhausen, M. Wieneke, W. Schwarz, *J. Organomet. Chem.* **1996**, *522*, 137–146.
- [23] M. Westerhausen, T. Bollwein, K. Polborn, *Z. Naturforsch.* **2000**, *55b*, 51–59.
- [24] M. A. Khan, D. G. Tuck, *Acta Crystallogr.* **1984**, *C40*, 60–62.
- [25] W. L. Steffen, G. J. Palenik, *Inorg. Chem.* **1977**, *16*, 1119–1127.
- [26] D.-M. Chen, X.-J. Ma, B. Tu, W.-J. Feng, Z.-M. Jin, *Acta Crystallogr.* **2006**, *E62*, m3174–m3175.
- [27] C. A. Haasnoot, F. A. A. M. de Leeuw, C. Altona, *Tetrahedron*, **1980**, *36*, 2783–2792.
- [28] The following equation and parameters according to Haasnoot and coworkers were applied: $^3J'(H, H) = P_1 \cos^2 \phi + P_2 \cos \phi + P_3 + \sum \Delta \chi_i (P_4 + P_5 \cos^2(\xi_i \phi + P_6 |\Delta \chi_i|))$; with P_{1-6} empirical parameters ($P_1 = 13.24$, $P_2 = -0.91$, $P_3 = 0$, $P_4 = 0.53$, $P_5 = -2.41$, $P_6 = 15.5$), ϕ torsion or dihedral angle, $\Delta \chi_i$ electronegativity difference, $\xi_i = +1$ or -1 to address the relative orientation.
- [29] P. G. M. Wuts, T. W. Green, *Green's Protective Groups in Organic Synthesis* 4th ed., John Wiley & Sons, Hoboken, **2007**.
- [30] E. J. Corey, A. Venkateswarlu, *J. Am. Chem. Soc.* **1972**, *94*, 6190–6191.
- [31] M. Schulz, R. Debel, H. Görls, W. Plass, M. Westerhausen, *Inorg. Chim. Acta*, **2011**, *365*, 349–355.
- [32] Z. Otwinowski, W. Minor in *Methods in Enzymology*, Vol. 276, *Macromolecular Crystallography*, Part A (Eds.: C. W. Carter Jr., R. M. Sweet), Academic Press, New York, **1997**, pp. 307–326.

- [33] R. Hoof, COLLECT, Nonius KappaCCD Data Collection Software, Nonius BV, Delft (The Netherlands) **1997**.
- [34] G.M. Sheldrick, SHELXS-97, Program for the Solution of Crystal Structures, University of Göttingen, Göttingen (Germany) **1997**. See also: G.M. Sheldrick, *Acta Crystallogr.* **2008**, A64, 467–473.
- [35] G.M. Sheldrick, SHELXL-97, Program for the Refinement of Crystal Structures, University of Göttingen, Göttingen (Germany) **1997**. See also: G.M. Sheldrick, *Acta Crystallogr.* **2008**, A64, 112–122.